Ferrimagnetic Mixed-Valency and Mixed-Metal Tris(oxalato)iron(III) Compounds: Synthesis, Structure, and Magnetism

Corine Mathonière,† Christopher J. Nuttall, Simon G. Carling, and Peter Day*

Davy Faraday Research Laboratory, The Royal Institution of Great Britain, 21 Albemarle Street, London W1X 4BS, U.K.

Received June 7, 1995[⊗]

The synthesis and structural and magnetic characterization of 16 compounds $AM^{II}Fe^{III}(C_2O_4)_3$ (A = N(*n*-C_3H_7)$_4$, N(*n*-C_4H_9)$_4$, N(*n*-C_5H_{11})$_4$, P(*n*-C_4H_9)$_4$, P(C_6H_5)$_4$, N(*n*-C_4H_9)$_3$($C_6H_5CH_2$), (C_6H_5)$_3$PNP(C_6H_5)$_3$, As(C_6H_5)$_4$; M^{II} = Mn, Fe) are reported. X-ray powder diffraction profiles are indexed in *R*3c or its subgroup $P6_522$ or *P*6/*mmm* to derive unit cell constants. The structures of all the compounds consist of two-dimensional honeycomb networks $[M^{II}Fe^{III}(C_2O_4)_3^-]_\infty$. The M^{II} = Fe compounds behave as ferrimagnets with T_c between 33 and 48 K, but five exhibit a crossover from positive to negative magnetization near 30 K when cooled in a field of 10 mT. The compounds exhibiting this unusual magnetic behavior are those that have the highest T_c. Within the set N(*n*-$C_nH_{2n+1})_4Fe^{II}Fe^{III}(C_2O_4)_3$ (n = 3−5), T_c increases with interlayer separation and the low-temperature magnetization changes from positive (n = 3) to negative (n = 4, 5). In the M = Mn^{II} compounds, the in-plane cell parameter a_0 is ∼0.03 Å greater than in the corresponding M = Fe^{II} ones while the interlayer separation (c_0/6) is on average 0.08 Å smaller. All members of the M^{II} = Mn series have magnetic susceptibilities showing broad maxima at 55 K characteristic of two-dimensional antiferromagnetism, but the magnetization of several of the salts increases sharply below 27 K due to the onset of spin canting, the magnitude of which varies significantly with A.

Introduction

The occurrence of long-range magnetic order in lattices composed of molecular transition metal complexes has been attracting increasing attention in recent years.[1] Such compounds are of interest because they are insulating, and hence frequently transparent, and offer the opportunity of creating novel lattice architectures. They also offer the chemist the opportunity to investigate how magnetic exchange interactions are propagated through extended polyatomic ligands. Prominent among the latter is the ambidentate oxalate ion, and numerous dimeric and trimeric oxalate complexes have been prepared as models.[2] However, in view of their simplicity and potential magnetic interest, it is surprising that only in the last two years have infinitely extended networks based on transition metal oxalato complexes been prepared.[3] The crystal structures of compounds $AM^{II}Cr(C_2O_4)_3$ with M^{II} = Mn and A = N(*n*-C_4H_9)$_4$ and P(C_6H_5)$_4$ consist of infinitely extended sheets of hexagonal symmetry containing alternating Mn and Cr octahedrally coordinated on each side of every oxalato anion.[4,5] The N(*n*-C_4H_9)$_4$ compounds show transitions to long-range magnetic order at temperatures between 6 and 14 K depending on M^{II}.[3]

In the search for chemical correlations between structure and properties in this interesting class of compounds, an important aspect is to extend the range of examples from four points of view. First, since they form layer structures, systematically varying A should modulate the separation between the layers, and hence the physical properties. Second, in view of the fact that three-dimensional as well as layer compounds of the type $AMM'(C_2O_4)_3$ have been reported,[4] it is important to delineate the extent to which the template cation A determines the crystal chemistry. Third, varying M^{III} as well as M^{II} gains access to a wider range of magnetic behavior; in particular, replacing Cr^{III} (S = $^3/_2$) with Fe^{III} (S = $^5/_2$) increases the moment and hence alters the ordering temperature, which scales with $JS(M^{II})\cdot S(M^{III})$, though of course J itself is sensitive to the orbital occupancy and the numbers of exchange pathways. Finally, in an earlier paper[6] we reported that N(*n*-$C_4H_9)_4Fe^{II}Fe^{III}(C_2O_4)_3$ exhibits a giant negative magnetization at low temperature unprecedented in molecular-based magnetic materials. It is therefore of great interest to find out how widespread this phenomenon is and whether a connection can be drawn with the cation A.

With these four issues in mind, we have therefore prepared polycrystalline samples of $AM^{II}Fe^{III}(C_2O_4)_3$ with layer structures analogous to those of $AMnCr(C_2O_4)_3$ (A = N(*n*-C_4H_9)$_4$, P(C_6H_5)$_4$), which have been determined.[4,5] Eight phases with different A are reported, each with M^{II} = Fe and Mn. The former are interesting because they are mixed-valency materials[7] while the latter are unusual in containing two different elements having the same electron configuration (high-spin $3d^5$). The crystallographic cell parameters were refined by least-squares-fitting X-ray powder diffraction data, and the susceptibilities and magnetizations were determined from 4 to 300 K. Several further examples of giant negative magnetization at low temperature have been found in the M^{II} = Fe series, and a qualitative explanation for the phenomenon is given in terms of the molecular field approach to ferrimagnetism.

* Corresponding author. FAX: +44 71 629 3569.
† Present address: Labo des Science Moléculaires, ICMCB, Chateau de Brivazac, Avenue du Dr. A. Schweitzer, 33608 Pessac Cedex, France.
⊗ Abstract published in *Advance ACS Abstracts,* February 1, 1996.

(1) See e.g.: Kahn, O., Molecular Magnetism; VCH: New York, 1994.
(2) Julve, M.; Fans, J.; Verdaguer, M.; Gleizes, A. *J. Am. Chem. Soc.* **1984**, *106*, 8306. Pei, Y.; Journeax, Y.; Kahn, O. *Inorg. Chem.* **1989**, *28*, 100.
(3) Zhong, Z. J.; Matsumoto, N.; Okawa, H.; Kida, S. *Chem. Lett.* **1990**, 87. Tamaki, H.; Mitsumi, M.; Nakamura, K.; Matsumoto, N.; Kida, S.; Okawa, H.; Iijima, S. *Chem. Lett.* **1992**, 1975. Tamaki, H.; Zhong, Z. J.; Matsumoto, N.; Kida, S.; Koikawa, N.; Achiwa, Y.; Hashimoto, Y.; Okawa, H. *J. Am. Chem. Soc.* **1992**, *114*, 6974.
(4) Decurtins, S.; Schmalle, H. W.; Oswald, H. R.; Linden, A.; Ensling, J.; Gütlich, P.; Hauser, A. *Inorg. Chim. Acta* **1994**, *216*, 65.
(5) Atovmyan, L. O.; Shilov, G. V.; Lyubovskaya, R. N.; Zhilyaeva, E. I.; Ovanesyan, N. S.; Pirumova, S. I.; Gusakovskaya, I. G. *JETP Lett.* **1993**, *58*, 766.
(6) Mathonière, C.; Carling, S. G.; Dou, Y.; Day, P. *J. Chem. Soc., Chem. Commun.* **1994**, 1551.
(7) Robin, M. B.; Day, P. *Adv. Inorg. Chem. Radiochem.* **1967**, *10*, 248. Day, P. *Int. Rev. Phys. Chem.* **1981**, *1*, 149.

0020-1669/96/1335-1201$12.00/0

Table 1. Refined Unit Cell Constants of $AM^{II}Fe^{III}(C_2O_4)_3$ (**1**−**8**, M^{II} = Fe; **9**−**16**, M^{II} = Mn)

compd	A	a_0, Å	c_0, Å	no. of peaks fitted
1	$N(n\text{-}C_3H_7)_4$	9.334(2)	49.31(3)	14
2	$N(n\text{-}C_4H_9)_4$	9.402(3)	53.88(5)	17
3	$N(n\text{-}C_5H_{11})_4$	9.406(6)	61.4(2)	13[a]
4	$P(C_6H_5)_4$	9.375(4)	57.45(5)	15
5	$N(C_6H_5CH_2)(n\text{-}C_4H_9)_3$	9.38(2)	57.8(2)	12[b]
6	$(C_6H_5)_3PNP(C_6H_5)_3$	9.38(1)	86.6(2)	13[b]
7	$P(n\text{-}C_4H_9)_4$	9.47(1)	55.9(2)	8
8	$As(C_6H_5)_4$	9.365(2)	57.93(4)	12
9	$N(n\text{-}C_3H_7)_4$	9.372(3)	49.11(6)	16
10	$N(n\text{-}C_4H_9)_4$	9.461(2)	53.62	17
11	$N(n\text{-}C_5H_{11})_4$	9.457(5)	60.95(1)	11[a]
12	$P(C_6H_5)_4$	9.428(4)	57.15(1)	11
13	$N(C_6H_5CH_2)(n\text{-}C_4H_9)_3$	9.470(4)	56.6(1)	12
14	$(C_6H_5)_3PNP(C_6H_5)_3$	9.413(3)	87.1(2)	13[b]
15	$P(n\text{-}C_4H_9)_4$	9.52(5)	55.17(8)	11
16	$As(C_6H_5)_4$	9.445(6)	57.4(1)	9

[a] $P6_522$. [b] $P6/mmm$.

Experimental Section

Chemicals were standard reagents from Aldrich (99% or higher purity). Solvents were reagent grade, deoxygenated where necessary by freeze−thaw cycles under vacuum. All manipulations of air-sensitive compounds were carried out by standard Schlenk techniques or in a N_2 dry box. N_2 was purified through columns containing BTS catalyst and 5 Å molecular sieves.

Elemental analyses were performed by the Microanalytical Departments at the Inorganic Chemistry Laboratory, Oxford, and University College, London.

X-ray powder diffraction profiles were recorded at room temperature on a Siemens D500 diffractometer in reflection mode using Cu Kα radiation with the monochromator set at 30° takeoff angle. Magnetic susceptibility and magnetization measurements were made using a Quantum Design MPMS 7 SQUID magnetometer. Polycrystalline samples were contained within gelatin capsules. The customary measuring protocol was to cool the sample in a field of 10 mT from ambient temperature to 2 K and record the susceptibility while warming. To estimate the Curie and Weiss constants, data from 150 to 300 K were used in every case. To render the results more comparable, the same number of data points and similar sample masses were employed. Correction for core diamagnetism of the sample was made using Pascal's constants and for the sample capsule by comparison with a standard measurement.

In a typical preparation, an aqueous solution (5 mL) of $K_3Fe(C_2O_4)_3 \cdot 3H_2O$[8] is added to an aqueous solution (5 mL) of $FeSO_4 \cdot 7H_2O$ or $MnSO_4 \cdot 7H_2O$ with stirring at room temperature. After 30 min, the solution is filtered to remove the small amount of $Fe(C_2O_4) \cdot 2H_2O$ which forms, and a methanol solution (5 mL) of AX (X = halide) is added to the filtrate, whereupon a precipitate begins to form. The solution is left for a period at room temperature before filtering. Optimum quantities of reagents and the reaction times are different for different A, varying from 1 to 2 mmol and from 1 h to several days, respectively. The longer the precipitation time, the less crystalline the resulting product is, as determined by XRD.

The following compounds were prepared in this way: for M^{II} = Fe, A = $N(n\text{-}C_3H_7)_4$ (**1**), $N(n\text{-}C_4H_9)_4$ (**2**), $N(n\text{-}C_5H_{11})_4$ (**3**), $P(C_6H_5)_4$ (**4**), $N(C_6H_5CH_2)(n\text{-}C_4H_9)_3$ (**5**), $(C_6H_5)_3PNP(C_6H_5)_3$ (**6**), $P(n\text{-}C_4H_9)_4$ (**7**), $As(C_6H_5)_4$ (**8**); M^{II} = Mn, with the same sequence of cations, compounds numbered **9**−**16** (Table 1). Elemental analyses showed that all the products had the formula $AM^{II}Fe(C_2O_4)_3$. The analytical data are available as Supporting Information. Attempts to prepare similar compounds with several other cations A were unsuccessful, as follows: $N(n\text{-}C_nH_{2n+1})_4$ (n = 1, 2, 6, 7), $N(n\text{-}C_{16}H_{33})(CH_3)_3$, and $P(C_6H_5)_3H$.

An alternative preparative route is to generate the $Fe(C_2O_4)_3^{3-}$ complex *in situ*. An aqueous solution (5 mL) of $FeCl_3 \cdot 6H_2O$ is added to one (5 mL) of $FeSO_4 \cdot 7H_2O$, and an aqueous solution (3 mmol in 5 mL) of oxalic acid is added dropwise. Upon addition of 5 mL of an aqueous or methanolic solution of $N(n\text{-}C_4H_9)_4I$, a green precipitate of **2** is formed immediately. It is also possible to carry out the reaction entirely in methanol solution.

(8) Bailar, J. C.; Jones, E. M. *Inorg. Synth.* **1939**, *1*, 37.

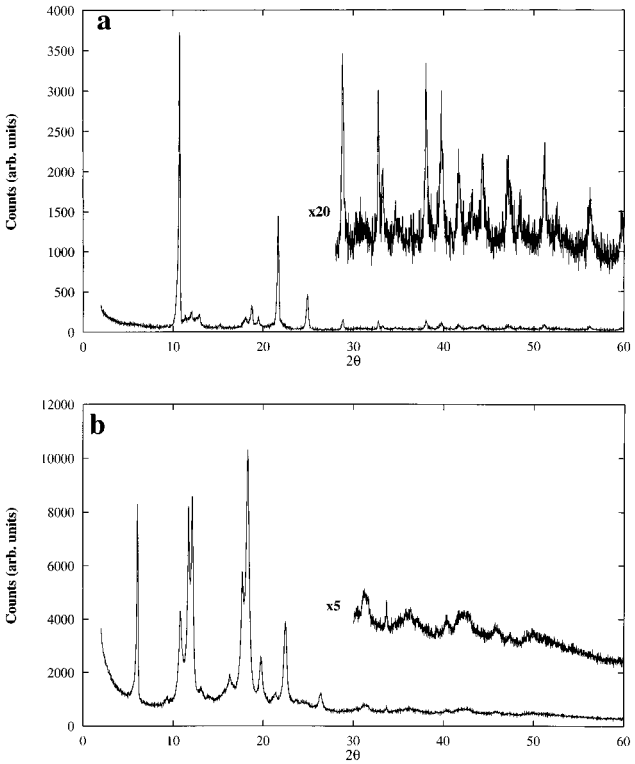

Figure 1. X-ray powder diffraction profiles for $AMn^{II}Fe^{III}(C_2O_4)_3$. A: (a) $N(n\text{-}C_3H_7)_4$; (b) $(C_6H_5)_3PNP(C_6H_5)_3$.

Crystals of **9**, were also prepared by placing 1 or 2 mmol of $K_3Fe(C_2O_4)_3$ and $MnSO_4 \cdot 7H_2O$ in one arm of an H-shaped tube and 1 mmol of $N(n\text{-}C_3H_7)_4Cl$ in the other, filling the cell carefully with water to prevent mixing, and allowing the reactants to diffuse together over a 2 month period.

Results

Crystal Structures. All the phases prepared were characterized by X-ray powder diffraction. In some preparations, peaks assignable to a few percent of $Fe(C_2O_4) \cdot 2H_2O$ were visible, but filtering the mixed M^{2+}, Fe^{3+}, $C_2O_4^{2-}$ solution before adding the A^+ eliminated them. Typical diffraction profiles are shown in Figure 1. For each compound, the reflections were indexed and unit cell constants were refined on a hexagonal cell as reported in refs 4 and 5. The values of the cell constants obtained are listed in Table 1. That the lattice constants in the basal plane are all so similar shows that the structures of all the compounds are similar and resemble those found by X-ray single-crystal diffraction for $AMnCr(C_2O_4)_3$ with A = $P(C_6H_5)_4$[4] and $N(n\text{-}C_4H_9)_4$.[5] However, varying the organic cation changes the spacing between the layers as anticipated. The structures of the $Mn^{II}Fe^{III}$ and $Fe^{II}Fe^{III}$ series correlate closely, as indicated by the cell parameters c_0 plotted in Figure 2a. The a_0 cell parameter varies little, as expected (Table 1 and Figure 2b). Refinement of the unit cell parameters for compounds **1**, **2**, **4**, **7**−**10**, **12**, **15**, and **16** was successfully accomplished within the space group $R3c$ assumed in refs 4 and 5. [We were informed by a reviewer that the structure of a compound **10** has been refined from single-crystal X-ray data in the space group $P6_3$ (Decurtins, S.; et al. Manuscript in preparation). However, for comparison with the other compounds, we use the larger hexagonal supercell.] However in several other cases, attempts to refine the cell constants in this space group left a number of intense peaks unassigned. The latter could only be fitted by assuming a lower symmetry space group, $P6_522$ for compounds **3** and **11** and $P6/mmm$ for compounds **5**, **6**, **13**, and

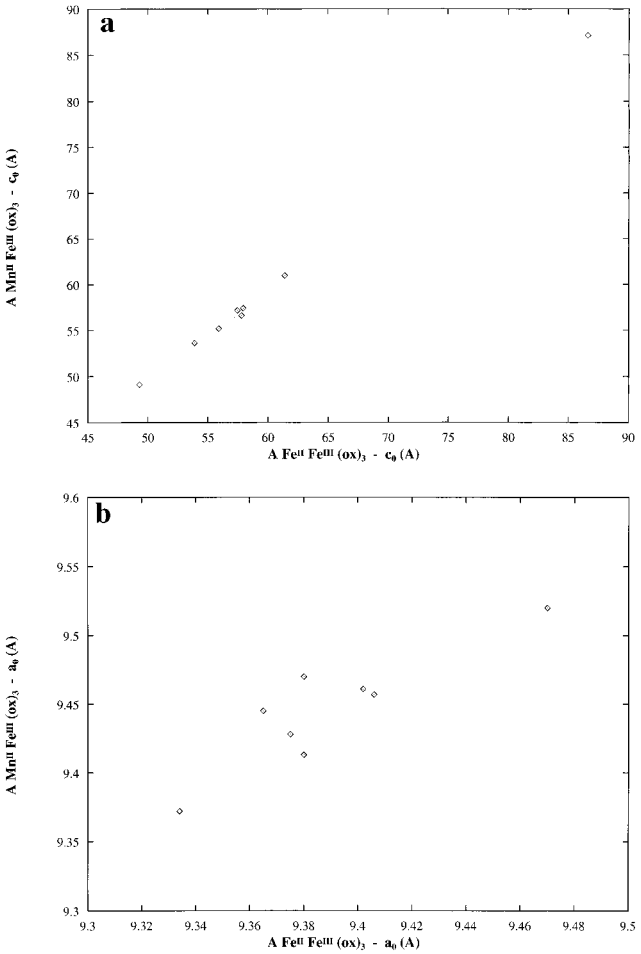

Figure 2. Unit cell parameters of $AM^{II}Fe^{III}(C_2O_4)_3$ (M = Mn^{II}, Fe^{II}): (a) c_0; (b) a_0. For numbering of compounds, see text.

14. In all three space groups, the separation between $MM'(C_2O_4)_3^-$ layers is $c_0/6$ so cation variation induces a change from 8.18 Å ($Mn^{II}Fe^{III}$) and 8.22 Å ($Fe^{II}Fe^{III}$) in the $N(n\text{-}C_3H_7)_4$ compounds, the smallest separation observed, to 14.52 Å ($Mn^{II}Fe^{III}$) and 14.43 Å ($Fe^{II}Fe^{III}$) in $(C_6H_5)_3PNP(C_6H_5)_3$, the largest found so far.

Magnetic Properties. The magnetic susceptibilities of polycrystalline samples of all the compounds, measured in a field of 10 mT, closely obeyed the Curie−Weiss law between room temperature and 150 K. The values of Curie (C) and Weiss constants (Θ) extracted by least-squares-fitting the data after subtraction of a correction for diamagnetism are listed in Table 2. The large negative values of the Weiss constants clearly indicate antiferromagnetic interaction between Mn^{II} or Fe^{II} and Fe^{III} in every case. In the $Fe^{II}Fe^{III}$ series, the values of Θ vary markedly with A, but among the $Mn^{II}Fe^{III}$ compounds, they span a smaller range, indicating that the near-neighbor exchange pathway is less sensitive to a change of organic cation. This is to be expected from the similar values of the unit cell parameter a_0.

Below 100 K the behavior of the $Mn^{II}Fe^{III}$ and $Fe^{II}Fe^{III}$ compounds must be examined separately. Considering first the $Fe^{II}Fe^{III}$ series, the compounds fall into two sets with sharply contrasting behavior. Adopting the measurement protocol defined in the Experimental Section, we find that in compounds **1**, **4**, and **8** the magnetization increases abruptly at 35, 37, and 33 K, respectively, corresponding to the onset of long-range order, increasing further in a conventional monotonic fashion down to 4 K (Figure 3). In striking contrast, in compounds **2**, **3**, and **5**−**7**, the onset of sharply increasing magnetization occurs at higher temperature (between 44 and 48 K), while at lower temperature the magnetization reaches a maximum, followed by a monotonic decrease down to 4 K, becoming strongly negative below about 30 K (Figure 3). This remarkable behavior is observed consistently in numerous samples, including ones which had been prepared by the *in situ* synthesis of $Fe(C_2O_4)_3^{3-}$ rather from previously prepared $K_3Fe(C_2O_4)_3$. It is discussed further below.

Table 2. Magnetic Parameters of $AM^{II}Fe^{III}(C_2O_4)_3$[a]

compd	T_c, K	Curie const C, emu K mol^{-1}	Weiss const Θ, K	negative magnetizn
1	35	8.0	−97	no
2	45	9.5	−120	yes
3	48	7.1	−140	yes
4	37	6.3	−86	no
5	44	7.7	−102	yes
6	45	10.2	−146	yes
7	45	8.5	−106	yes
8	33	7.3	−113	no
9	28	10.4	−127	
10	28	10.6	−121	
11	27	10.5	−124	
12	25	8.9	−128	
13	26	9.6	−117	
14	29	10.3	−136	
15	26	8.9	−124	
16	27	10.6	−122	

[a] For numbering of compounds, see text.

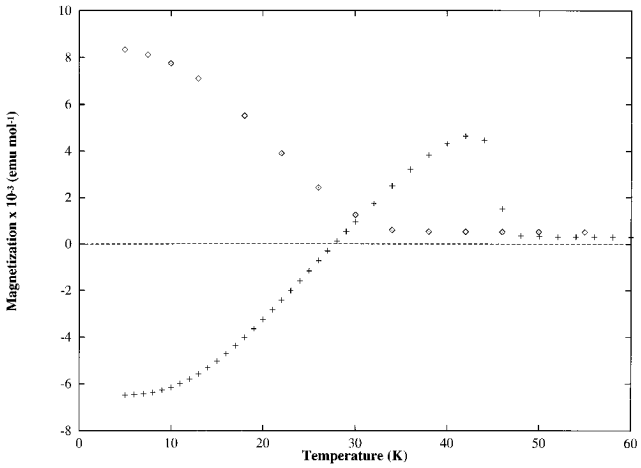

Figure 3. Temperature dependence of the magnetization of $AFe^{II}Fe^{III}(C_2O_4)_3$ in a field of 10 mT: (◇) $As(C_6H_5)_3$; (+) $(C_6H_5)_3PNP(C_6H_5)_3$.

From room temperature to 150 K, the susceptibilities of polycrystalline samples of the $Mn^{II}Fe^{III}$ compounds likewise obey the Curie−Weiss Law, with negative Weiss constants indicating near-neighbor antiferromagnetic exchange. At lower temperature, the susceptibilities pass through a broad maximum near 55 K of the kind seen in low-dimensional antiferromagnets. In the $P(C_6H_5)_4$ compound **12**, the susceptibility below 55 K continues to fall monotonically to below 10 K, but in the other $Mn^{II}Fe^{III}$ compounds, there is a discontinuous jump in susceptibility at 27 K (Figure 5), suggesting the onset of spin canting. A small single crystal of **9** was studied as a function of temperature at applied magnetic fields of 100, 500, and 1000 G with the results shown in Figure 6. It is apparent from the single-crystal data that the 27 K transition is not first but second order.

Discussion

Crystal Chemistry. The existence of such a large number of compounds sharing the stoichiometry $AM^{II}Fe^{III}(C_2O_4)_3$ invites discussion of their crystal chemistry as a prelude to rationalizing their magnetic properties. Since the full structure cannot be resolved from powder X-ray data, we base the discussion on the variation in the unit cell parameters.

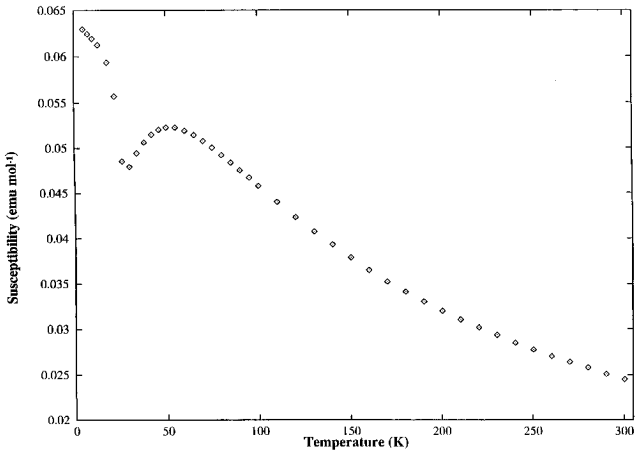

Figure 4. Temperature dependence of the susceptibility of polycrystalline $N(n\text{-}C_4H_9)_4Mn^{II}Fe^{III}(C_2O_4)_3$ from 10 to 300 K.

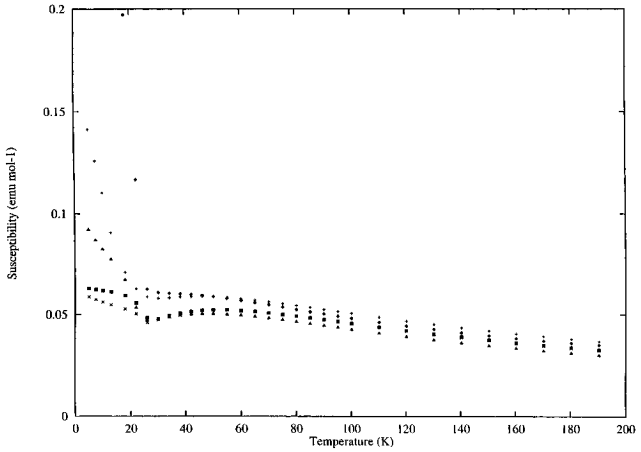

Figure 5. Temperature dependence of the susceptibility of several polycrystalline $AMn^{II}Fe^{III}(C_2O_4)_3$ compounds showing spin canting at low temperature: (◆) $(C_6H_5)_3PNP(C_6H_5)_3$; (+) $As(C_6H_5)_4$; (▲) $(C_6H_5\text{-}CH_2)N(n\text{-}C_4H_9)_3$; (■) $N(n\text{-}C_4H_9)_4$; (×) $P(n\text{-}C_4H_9)_4$.

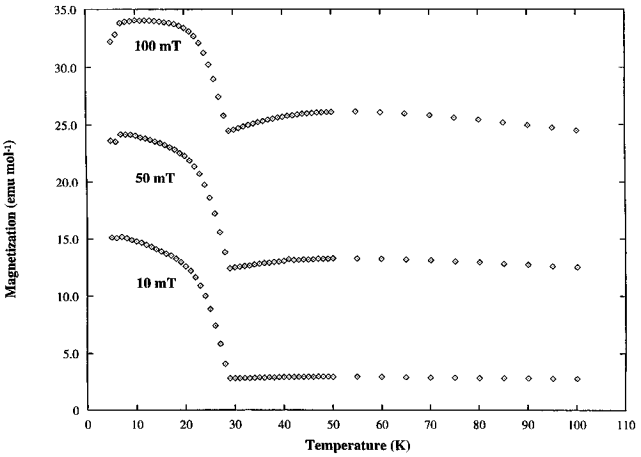

Figure 6. Temperature dependence of the magnetization of a single crystal of $N(n\text{-}C_3H_7)_4Mn^{II}Fe^{III}(C_2O_4)_3$ in fields of 10, 50, and 100 mT.

On the basis of model building and topological arguments, it is possible to envisage two modes of connectivity between octahedral tris-bidentate $M^{III}(C_2O_4)_3^{3-}$ groups mediated by M^{II}, each of which in turn is coordinated by three octahedrally disposed (C_2O_4).[2,3] These two modes correspond to each octahedron being connected to its neighbors through three edges. If, in a trigonally distorted octahedron having D_3 symmetry, the edges in question are related by a 3-fold screw axis, polymerization can take place, in principle, in two ways. One alternative leads to an infinite honeycomb layer in which the 3-fold screw axes of all the octahedra are aligned perpendicular

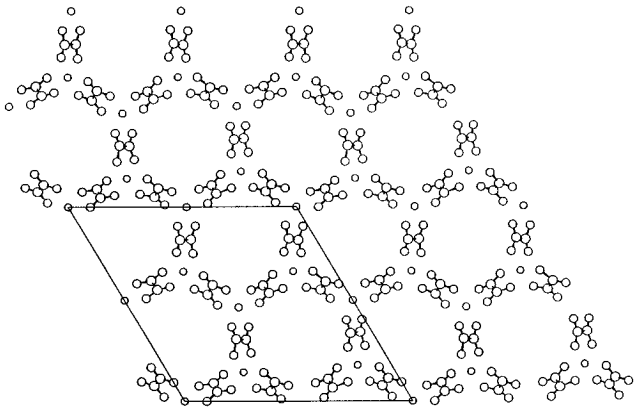

Figure 7. The honeycomb layer arrangement of $[MM'(C_2O_4)_3]^-$.

to the plane (Figure 7). In the other possible arrangement, the octahedra are connected in helical ribbons so that their 4-fold axes are all aligned. The crystal structures of two examples of $AMM'(C_2O_4)_3$ compounds containing monopositive A cations determined to date both reveal honeycomb layer arrangements.[4,5] On the other hand, when $A = [Fe(bipy)_3]^{2+}$ and $M = M' = Fe^{II}$, a cubic lattice is found ($P4_332$) with the second form of connectivity.[9] Clearly, therefore, the organic cation A^+ is capable of acting as a template to direct the polymerization in a manner analogous to zeolites.

All the template cations A used in the present work are of quaternary ammonium, phosphonium, or arsonium type. They give rise to compounds having a layer honeycomb structure, although they include both alkyl- and phenyl-substituted species as well as one containing the two types of substituent together. Equally of interest is the range of XR_4^+ for which no bimetallic tris(oxalato) compounds could be synthesized. For example in the $N(n\text{-}C_nH_{2n+1})_4^+$ sequence for $n = 1-7$, only $n = 3-5$ gave crystalline products, while highly asymmetrically substituted species such as the surfactant $(C_{16}H_{33})N(CH_3)_3^+$ and $(C_6H_5)_3\text{-}PH^+$ did not.

In the crystal structure of $P(C_6H_5)_4MnCr(C_2O_4)_3$, the organic cations occupy sites interleaved between the $[MnCr(C_2O_4)_3]_\infty$ layers in such a way that one P−C bond of each cation lies parallel to the 3-fold axis of the hexagonal unit cell, i.e. perpendicular to the anion layer. The C_6H_5 ring in question resides within the cavity formed by six $(C_2O_4)^{2-}$ while the remaining three extend between the anion layer.[4] Unfortunately the only N and one C atom of the organic cations were located in the structure determination of $N(n\text{-}C_4H_9)_4MnCr(C_2O_4)_3$[5] though the assumption of the $R3c$ space group requires the N to be placed on a 3-fold axis with one C−N bond parallel to the axis. The remaining C atoms were assumed to be fully disordered. A reasonable hypothesis, however, is that one C_4H_9 chain extends into the cavity in the $[MnCr(C_2O_4)_3]_\infty$ layer in a fashion analogous to the phenyl group in the $P(C_6H_5)_4$ compound. On that basis, the increments of interlayer spacing in the $N(n\text{-}C_nH_{2n+1})_4$ compounds for $n = 3-4$ and $4-5$ ought to correspond to the interpolation of a C−C bond. The increments in question are respectively 0.76 and 1.25 Å in the $Fe^{II}Fe^{III}$ case and 0.75 and 1.22 Å in the $Mn^{II}Fe^{III}$.

The increments in c_0 correspond precisely to the well-known "alternation effect" in the unit cell constants of *n*-alkanes or compounds containing extended aliphatic hydrocarbon chains such as the layer perovskite halide salts $(n\text{-}C_nH_{2n+1}NH_3)_2MX_4$.[10] In the latter, the increment in interlayer spacing on extending the chain by one CH_2 unit is smaller when one passes from odd to even than when one passes from even to odd, exactly as

(9) Decurtins, S.; Schmalle, H. W.; Schneuwly, P.; Ensling, J.; Gütlich, P. *J. Am. Chem. Soc.* **1994**, *116*, 9521.

found here. Indeed, adopting the same geometrical argument as in other organic−inorganic layer systems,[11,12] we can use the observed increments to estimate the angle that the N−C bond of A^+ in the present series makes with the $[M^{II}Fe(C_2O_4)_3^-]_\infty$ layer. With the C_nH_{2n+1} chains fully extended, and taking the C−C bond length as 1.54 Å and the C−C−C angle as the normal tetrahedral one, the "axial" C−C bonds make angles of approximately 60° with the anion layer. The a_0 parameters also increase from $n = 3$ to $n = 4$ by 0.07 and 0.09 Å (Fe^{II} and Mn^{II}) but remain constant within experimental error from $n = 4$ to $n = 5$. On the other hand, there is a marked increase in a_0 (0.06 Å) from $N(n\text{-}C_4H_9)_4$ to $P(n\text{-}C_4H_9)_4$, the latter having the largest a_0 of the series. For comparison, the difference in N−C and P−C bond lengths is 0.36 Å. Finally, it is significant that the *c*-axis parameters of the $P(C_6H_5)_4$ and $N(C_6H_5CH_2)(n\text{-}C_4H_9)_3$ compounds are almost equal, suggesting that in both cases the plane of a phenyl group is aligned perpendicular to the anion layer.

In view of the large number of new compounds $AM^{II}Fe(C_2O_4)_3$ reported in Table 1, further structural correlations can be established. The $Mn^{II}Fe^{III}$ and $Fe^{II}Fe^{III}$ compounds containing the same A^+ are isostructural, but while the c_0 cell parameters in the two series correlate closely (Figure 2a), examination of the *a* parameters shows that the correlation is less precise (Figure 2b). However, in every case, the parameter a_0 of the $Mn^{II}Fe^{III}$ compound is larger than that of the corresponding $Fe^{II}Fe^{III}$ one, the mean difference among eight A being 0.054 Å. By contrast, for all A except $(C_6H_5)_3PNP(C_6H_5)_3$ (compounds **6** and **14**), the c_0 parameter of the $Mn^{II}Fe^{III}$ compound is smaller than the corresponding $Fe^{II}Fe^{III}$ one, by an average of 0.50 Å, i.e. a difference in interlayer spacing of 0.083 Å. The variation in a_0 is sufficiently explained by a decrease in size of M^{II} from Mn to Fe, the ionic radii being respectively 0.82 and 0.77 Å.[13] On the other hand, we explain the change in c_0 by noting that expanding the hexagonal cavities in the $[M^{II}Fe(C_2O_4)_3]_\infty$ layers on replacing Fe^{II} by Mn^{II} permits the alkyl or aryl side chain of the A^+ to enter further, thus creating a more densely packed structure.

Magnetic Properties. We consider first the $Fe^{II}Fe^{III}$ series. Referring to the data in the paramagnetic region, the mean value of the measured Curie constant (8.0 emu K mol^{-1}) is consistent with the presence of high-spin Fe^{II} and Fe^{III}, the value of *C* calculated on the assumption $S(Fe^{III}) = {}^5/_2$, $S(Fe^{II}) = 2$, and $g = 2$ for both ions being 7.4 emu K mol^{-1}. The measured Curie and Weiss constants span a wide range, the largest values of *C* being (with one exception) correlated with the largest Θ (Table 2). This can be explained by noting that the highest measurement temperature accessible in the present study was 300 K, i.e. only 2−3Θ, so it is arguable that the true Curie−Weiss regime has not been accessed. Second, the Fe^{II} ground state is complex, since the degeneracy of the cubic field $^5T_{2g}$ term is lifted, not only by first-order spin−orbit coupling but also by a trigonal field component, which can also vary with the organic template cation. Furthermore, the spin−orbit coupling constant of Fe^{II} is comparable in magnitude to *kT* in the temperature range covered by the measurements,[14] so an orbital contribution to the observed moment is expected. It might be thought that the strong antiferromagnetic near-neighbor exchange indicated by the large negative values of Θ could be examined by considering the interactions between the orbitals carrying the unpaired electrons. However, the problem is greatly complicated by the presence of unquenched orbital angular momentum on one of the ions (Fe^{II}), and no generally applicable formalism for such a case has yet been given (see ref 1, section 9.6).

A subset of the $Fe^{II}Fe^{III}$ series that permits some precise magneto−structural correlations is the one with $A = N(n\text{-}C_nH_{2n+1})_4$ having $n = 3-5$, in which there is a monotonic increase in Θ and T_c with increasing *n*, i.e. with increasing c_0. Such a variation is extremely unusual, since for organic−inorganic layer compounds[15] in which inorganic magnetic layers are interleaved by aliphatic carbon chains, the 3D ordering temperatures (while not very sensitive to interlayer separation) universally decrease as the distance between the layers increases.[16,17] In the $Fe^{II}Fe^{III}$ series, there is a marked correlation between the measured Weiss constant Θ determined from the susceptibility in the paramagnetic region above the onset of long range order and the ordering temperature T_c, those compounds having the largest Θ also having the highest T_c (Table 2). The existence of that correlation requires that exchange between metal ions in neighboring layers is important, as well as exchange within the layers. Consequently, though the crystal structure is clearly two-dimensional, the exchange interactions are not. More detailed experiments on single crystals will be needed to clarify the issue.

The most striking feature of the magnetic behavior of the $Fe^{II}Fe^{III}$ series is the occurrence of apparently negative magnetization at low temperature. We found this phenomenon in the $N(n\text{-}C_4H_9)_4$ compound,[6] but the extended series of examples reported in the present paper enables us to confirm that it is a widespread but not universal feature of this class of material. Such behavior is unprecedented in molecular-based magnets, though cases have been known for many years in the ferrites[17,18] where the concentration of magnetic ions on the tetrahedral (A) and octahedral (B) sites in the AB_2O_4 spinel lattice may vary as a result of forming solid solutions, e.g. in $NiFe_{2-x}V_xO_4$ where the cation distribution is $Fe[NiFe_{1-x}V_x])O_4$.[17] In his classic theory of ferrimagnets, Neel[19] envisaged the possibility that the spontaneous magnetization might change sign at a so-called "compensation temperature" T_{comp}, when the net magnetizations of the two sublattices cancelled each other. The phenomenon can arise when the two sublattice magnetizations have different temperature dependences. The situation is shown schematically in Figure 8. Since the Fe^{III} ground state is orbitally nondegenerate, the magnetization of the Fe^{III} sublattice follows a Brillouin curve in the molecular field approximation, but in view of its orbital degeneracy, that of the Fe^{II} will not. Furthermore, the Fe^{II} ion shows single-ion anisotropy due to spin−orbit coupling so the orientation of the Fe^{III} moments is pinned to the Fe^{II} should the latter exert the larger molecular field in the temperature range immediately below T_c.

Evidence that the Fe^{II} and Fe^{III} sublattices do not become magnetized to an equivalent extent at the same temperature comes from temperature-dependent Mössbauer spectroscopy. At 4.2 K compound **2** shows a six-line Fe^{III} spectrum corresponding to an internal field of 53 T, while the Fe^{II} component of the spectrum was fitted to an internal field of only 4 T, though the analysis was complicated by an impurity of a few percent $Fe(C_2O_4)\cdot 2H_2O$.[20] Temperature-dependent measurements on a sample of **2** uncontaminated by $Fe(C_2O_4)\cdot 2H_2O$ reveal that, while the internal field at the Fe^{III} site is clearly established at

(10) Arend, H.; Huber, W.; Mischgofsky, F. H.; Richter van-Leeuwen, G. K. *J. Cryst. Growth* **1978**, *42*, 213.
(11) Beneke, K.; Lagaly, G. *Clay Miner.* **1982**, *17*, 175.
(12) Buckley, A. M.; Bramwell, S. T.; Visser, D.; Day, P. *J. Solid State Chem.* **1987**, *69*, 240.
(13) Shannon, R. D.; Prewitt, W. *Acta Crystallogr.* **1969**, *B25*, 925.
(14) Figgis, B. N. *Introduction to Ligand Field Theory*; Interscience: New York, 1966.
(15) Day, P. *Philos. Trans. R. Soc.* **1985**, *A314*, 145.
(16) Bellitto, C.; Day, P. *J. Mater. Chem.* **1992**, *2*, 265.
(17) Blasse, G.; Gorter, E. W. *J. Phys. Soc. Jpn., Suppl. B-1* **1962**, *17*, 176. Gorter, E. W. *Philips Res. Rep.* **1954**, *9*, 403.
(18) Goodenough, J. B. *Magnetism and the Chemical Bond*; Interscience: New York, 1963.
(19) Neel, L. *Ann. Phys.* **1948**, *3*, 137.

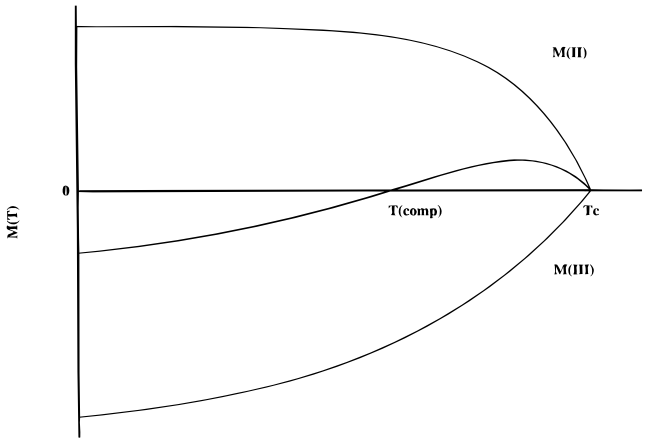

Figure 8. Temperature-dependent magnetization of a two-sublattice ferrimagnet, showing the occurrence of a compensation temperature T_{comp}.

35 K, the field at the Fe^{II} site is still small at 10 K.[21] Given the topology of the 2D honeycomb lattice (Figure 7), the largest component of the molecular field experienced by the Fe^{III} is due to the neighboring Fe^{II} and vice versa. Thus the Mössbauer results confirm the hypothesis that the Fe^{II} sublattice magnetization increases more steeply below T_c than that of the Fe^{II} sublattice. Qualitatively, therefore, the situation in those compounds exhibiting negative magnetization at low temperature must indeed be as shown in Figure 8.

Finally, we address the question of why some of the $AFe^{II}Fe^{III}(C_2O_4)_3$ compounds show negative low-temperature magnetization while others do not. First of all, reference to Tables 1 and 2 shows that the phenomenon is not confined to those compounds with either the smallest or the largest interlayer separation. On the other hand, the compounds showing the effect are those with the highest T_c and (with one exception (**5**)) the largest Θ. The first of these observations requires that something more than interlayer interaction is responsible, while the second reveals the importance of the magnitude of the near-neighbor exchange interaction. The latter is a function of the intraplanar cation−cation separation, as well as the "bite" angle subtended by the bidentate $C_2O_4^{2-}$ bridging group and the degree of trigonal distortion around the cation sites. The sign and magnitude of the trigonal distortion, which is modulated by the intercalated organic template cations A, also determine the single ion anisotropy at the Fe^{II} site, which in turn affects the temperature dependence of the spontaneous magnetization of the Fe^{II} sublattice. Definition of all these parameters must await a full set of crystal structure determinations. Other physical methods, especially neutron diffraction, will be required to determine the distribution of the cations and their moments in the $Fe^{II}Fe^{III}$ tris(oxalate) series, but a final observation from the present study should be noted. Although the samples were synthesized under anaerobic conditions, their elemental analyses reveal a small deficiency in Fe. This may be due to a small fraction of the Fe^{II} becoming oxidized to Fe^{III}, despite the anaerobic conditions. Thus the ratio of Fe^{II} to Fe^{III} may deviate slightly from the ideal of 1:1, introducing a small fraction of metal vacancies (cf. wustite, $Fe_{1-x}O$).

The magnetic properties of $Mn^{II}Fe^{III}$ tris(oxalate) series also reveal a number of highly unusual features. First, we have the unique situation that both metal ions have the same electronic ground state, $^6A_1$ in the D_3 point group. The Curie and Weiss constants (Table 2) span a much smaller range than those of the $Fe^{II}Fe^{III}$ series, though the former (mean value 10.0 emu K mol^{-1}) are larger than the value of 8.75 emu K mol^{-1} calculated for $S(Mn^{II}) = S(Fe^{III}) = {}^5/_2$ and $g = 2$. Likewise the T_c's vary only over about half the range as in the $Fe^{II}Fe^{III}$ series, with the same set of A. Apart from differences in the g values, which are very small since both ions have orbital singlet ground states, the compounds are expected to mimic antiferromagnetic rather than ferrimagnetic behavior. This is borne out by the temperature dependence of the susceptibility, which is indeed that of a classic 2D antiferromagnet,[22] reaching a broad maximum at 55 K. An example is shown in Figure 4, but similar behavior is found in all eight compounds studied, indicating that the in-plane near-neighbor exchange constant does not vary significantly with changing organic cation A. In contrast, the degree of spin canting evidenced by the sharp rise in magnetization below 27 K varies very markedly with organic cation. The magnitude of the uncompensated moment, as indicated by the magnetization at 5 K, increases in the sequence $N(n\text{-}C_4H_9)_4 \sim P(C_6H_5)_4 < P(n\text{-}C_4H_9)_4 < N(n\text{-}C_3H_7)_4 < As(C_6H_5)_4 < (C_6H_5)_3PNP(C_6H_5)_3$ (Figure 5). This order does not follow that of increasing interlayer separation (Table 1), so the spin canting arises from more subtle variations in the structure than those of the a_0 and c_0 parameters alone.

Conclusion

In this paper we have shown that 2D ferrimagnets $AM^{II}Fe^{III}(C_2O_4)_3$ (M^{II} = Mn, Fe) are formed by a wide variety of organic template cations A, giving material for extensive crystal chemical and magneto−structural correlation. In all, unit cell and magnetic parameters for 16 compounds are presented. In the series $N(n\text{-}C_nH_{2n+1})_4Fe^{II}Fe^{III}(C_2O_4)_3$ ($n = 3-5$), Θ and T_c *increase* with increasing n, as does the interlayer separation, the latter in the manner expected for intercalated *n*-alkyl groups. Several of the $Fe^{II}Fe^{III}$ compounds show negative magnetization at low temperature together with a "compensation temperature" at which the net magnetization vanishes, reminiscent of that found in ferrospinel solid solutions.[17] A qualitative explanation for the negative magnetization is found in Neel's theory of two-sublattice ferrimagnets.[19] This phenomenon is seen in the compounds with the largest measured Θ and T_c. Nevertheless there is no correlation between these magnetic parameters and interlayer separation. The corresponding $Mn^{II}Fe^{III}$ compounds mimic 2D antiferromagnets, though with a degree of spin canting at low temperature which varies strongly with the organic template cation. While the present work reveals many unusual features in the properties of the compounds $AM^{II}Fe^{III}(C_2O_4)_3$ with honeycomb layer structures, much remains to be done to understand the detailed relation of these properties with crystal structure, for which further X-ray and magnetic experiments with single crystals will be necessary. Our work is continuing in this direction.

Acknowledgment. We acknowledge the U.K. Engineering and Physical Sciences Research Council for an equipment grant and support to C.J.N. and S.G.C. and the European Union for an Institutional Fellowship (C.M.) and support through the Network on Molecular-based Magnets. We are grateful to Dr. J. Ensling (Mainz) for measuring Mossbauer spectra of compound **2** and to one of the reviewers for pointing out the unpublished structure determination of compound **10**.

Supporting Information Available: A table of analytical data for $AM^{II}Fe^{III}(C_2O_4)_3$ (1 page). Ordering information is given on any current masthead page.

IC950703V

(20) Iijima, S.; Katsura, T.; Tamaki, H.; Mitsumi, M.; Matsumoto, N.; Okawa, H. *Mol. Cryst. Liq. Cryst.* **1993**, *233*, 263. Reiff, W. M.; Kreisz, J.; Meda, L.; Kirss, R. U. *Mol. Cryst. Liq. Cryst.* **1995**, *273*, 181.

(21) Ensling, J. Personal communication.

(22) de Jongh, L. J.; Miedema, A. R. *Adv. Phys.* **1974**, *24*, 1.